Quality control and data flow operations of SPHERE

Wolfgang Hummel[a], Julien H.V. Girard[b], Julien Milli[b], Zahed Wahhaj[b], Lars Lundin[a], and Arthur Vigan[b,c]

[a]European Southern Observatory, Karl-Schwarzschild-Str. 2, D-85748 Garching, Germany
[b]European Southern Observatory, Alonso de Cordova 3107, Vitacura, Casilla 19001, Santiago 1 9, Chile
[c]Lab. d'Astrophysique de Marseille, CNRS, Aix Marseilles Univ. UMR 7326, 13388 Marseille, France

ABSTRACT

ESO operates since April 2015 the new planet finder instrument SPHERE[1] with three arms supported by a common path coronograph with extreme AO. Observing modes include dual band imaging, long slit spectroscopy, IFS and high contrast polarimetry. We report on the implementation of the SPHERE data flow and quality control system and on operational highlights in the first year of operations: This includes some unconventional parts of the SPHERE calibration plan like special rules for the selection of filters and the measures for an optimized calibration of the two polarimetric channels of the ZIMPOL arm. Finally we report on the significance of the SPHERE quality control system, its relation to the data reduction pipeline and which previously undocumented instrumental features have been revealed so far.

Keywords: SPHERE, quality control, data flow operations, NIR, calibration plan

1. INTRODUCTION

On April 2015 the new instrument SPHERE (Spectro-Polarimetric High contrast Explanet REsearch) was put in operation at UT3 of the ESO VLT. SPHERE consists of three arms: IRDIS (IR Differential Imaging Spectrometer), IFS (Integral Field Spectrometer) and ZIMPOL (Zurich IMaging POLarimeter), of which the first two arms can operate simultaneously. IRDIS offers classical imaging (CI), dual band imaging (DBI), differential polarimetric imaging (DPI) and long slit spectroscopy (LSS). IFS covers either the YJH bands or YJ bands alone where the K band or the HK bands can be observed simultaneously with IRDIS. ZIMPOL is an optical instrument with a 2-phase demodulation scheme synchronized with the modulated polarization orientation that allows for the quasi-simultaneous observations of both polarimetric orientations in the visual.

All three instrumental arms are fed by the Common Path Interface (CPI). Its main components are the high order deformable mirror that provides a stable AO-corrected image and the apodized Lyot stop coronograph for the NIR and the visual.

Each of the seven observing modes of the instrument (four in IRDIS, IFS and two in ZIMPOL) is calibrated according to a dedicated calibration plan.

SPHERE is one of the most complex instruments of the VLT both from the technical point of view as well as from the point of view of data flow and back end operations. Here we report on the implementation of the SPHERE calibration plans, the design and implementation of the quality control service and highlights during the first year of operations.

Further author information: (Send correspondence to W.H.)
W.H.: E-mail: whummel@eso.org, Telephone: +49 89 32006 728

2. IMPLEMENTATION OF THE SPHERE CALIBRATION PLAN

The starting point for embedding a new instrument within the VLT data flow is the calibration plan (hereafter CP) of the instrument. The entities of the CP are the raw frames generated by the instrument. The CP lists the kind of raw data types (e.g flat field frames, optical distortion calibrations or long slit spectroscopy science frames), and their identification via keyword values in the frame headers. Furthermore classified frames are grouped according to instrument setup properties. Finally the CP determines the associations between calibrations and calibrations and the associations between calibration and science frames and the corresponding matching constraints.

The CP has been implemented using the common OCA framework syntax[2] in the VLT data flow at several places in the data stream.

1. On site on Paranal as part of the online pipeline infrastructure. This implementation is to support science operations staff.
2. A reduced set of OCA rules is used off site in Garching for checking the completeness of calibrations via the *CalChecker*[*] tool.
3. The processing of calibrations via the off-line pipeline to provide master calibrations for the quality control service.
4. The *calSelector*[†] interface is to download science frames together with the required associations from the archive. The associations of calibrations are controlled via the OCA rules. Both variants: downloading the full cascade of raw calibrations (= raw2raw mode) and downloading master calibrations (= raw2master mode) are supported.
5. In addition OCA rules build the backbone of the *reflex*[3] work flow on the users desktop.

Each of these implementations follow different motivations. The implementation of the CPs as OCA rules for *calChecker* and *calSelector raw2raw* does not involve real master calibrations.

2.1 IRDIS

This instrument arm consists of four different modes of which the CPs of classical imaging, dual band imaging and differential polarimetric imaging are straightforward, meaning the logical sequence of dependencies can be organized in the same single chain. Long slit spectroscopy, which require arc frames and imaging flats can be organized in the same sequential logic. Fig. 1 shows a tabular representation of the CP for the IRDIS DBI mode.

2.2 IFS

The plan to calibrate the IFS arm of SPHERE is more complex, due to the lenslet format, the related cube reconstruction and the optical distortion calibrations. Furthermore imaging flats with up to four different internal laser lamps are acquired for the chromatic correction of the pixel responses. The first steps of the IFS CP are handling raw frames and products in the imaging plane, while later steps in the sequence operate on raw frames and products in the IFS format. The particular difficulty of the IFS CP in implementing the association rules in the OCA syntax is that the IFS spectral position calibration requires up to four calibrations of the same kind, but distinct setups.

There are usually different potential ways to solve such issues, when the design of the CP exceeds the complexity that can be handled within the OCA framework and the VLT data flow: a) upgrade the OCA framework, a solution which is very expensive, b) modify the calibration template which results in a more suitable organization of the raw frames or c) modify the design of the identification and organization of the expected calibration products.

[*] CalChecker: `www.eso.org/observing/dfo/quality/ALL/daily_cal.html`

[†] calSelector: `archive.eso.org/cms/application_support/calselectorInfo.html`

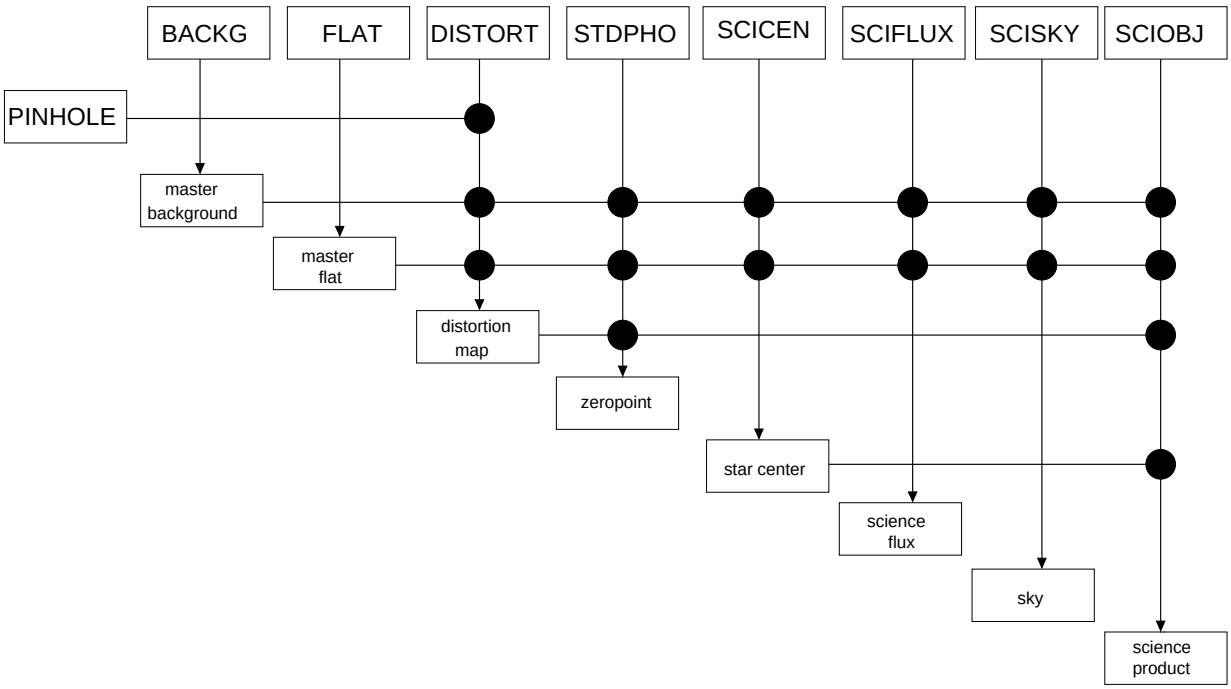

Figure 1. This Figure shows a tabular representation of the calibration plan of modes IRDIS CI, DBI and DPI. The first row lists the tags of the raw frame categories. The second row shows the static calibration, in this case the positions of the pinhole calibration mask. Horizontal lines mean associations and vertical lines mean processing steps. E.g. the generation of a optical distortion map product is triggered by a distortion raw frame (DISTORT). It requires the static calibration PINHOLE, a master background and a master flat. The black circles represent the matching constraints. E.g. the upper right black circle stands for the constraint, that the associated master background product must match the IRDIS broad band filter, the IRDIS dual band filter, the detector DIT and the CPI neutral density filter used for the science observation and the time match rule allows for up to one day time difference. The raw type tags SCICEN, SCIFLUX and SCISKY stand for attached calibrations. The lower right black circle stands for the constraint, that for the association of the star center observation the observation block ID must be matched and the closest in time should be used (in case the observations was repeated).

The problematic association occurs only in those association flavors, where real master calibrations are involved, hence in options 1), 3), 4) and 5) of section 2. A change request for the product header keys of the IFS detector flat recipe and the spectral position recipe resulted in proper classification and organization of the product frames.

2.3 ZIMPOL

While the dual beam filter wheel of IRDIS is technically a single wheel with slot pairs of fixed filter combinations, ZIMPOL has for each beam a separate filter wheel allowing for any filter combination in both channels with differing throughput ratios of up to a factor of five. Each channel has its own CCD, but both are operated by a common controller. While it makes sense to observe one target with filters of different throughput in both channels, a problem arises for the calibrations where one lamp is involved. Since the exposure is the same for both channels, a broad band filter flat might saturate in one channel while the narrow band filter flat with lower throughput in the other channel not yet achieved the requires signal to noise ratio.

A further peculiarity of ZIMPOL is, that the raw frames consist of two detector extensions, while the pipeline products generate for each detector an individual file. This means that not only the data format changes during the processing of the calibration cascade but also the the way the pixel data are encapsulated.

Both challenges required several iterations within the project team. The first issue was solved by Paranal Science Operations by providing lamp calibrations of distinct throughput with sufficient counts in both channels

and for the second ZIMPOL peculiarity the pipeline product pairs are handled as a single entity (like a single raw frame) within the data flow, meaning the detector is handled once as an instrument setup and once as product category.

For several IRDIS and ZIMPOL modes it is justified to calibrate narrow band filter science frames with broad band filter calibrations as long as the narrow band filter wavelength range is covered by the broad band filter wavelength range. Therefore some time expensive calibrations are acquired in a limited set broad band filters only. These synergies were identified in a later phase of the design of the SPHERE operation plan. Since the raw frame headers do bot contain related header keys to group frames according to broad band ranges, the association is implemented by a cumbersome but accurate rule within the OCA framework.

3. OPERATIONAL HIGHLIGHTS OF QUALITY CONTROL

Within the VLT data flow model astronomical data quality control is a shared task between the Science Operations department on Paranal and the Quality Control and Data Processing group at ESO headquarters in Garching.[7] While the QC on site focus on spot checks on the raw data and is checking the observation constraint sets against the actual ambient conditions and lunar constraints, off-site QC focus on pipeline processed master calibrations. This scheme has been in operations for more than fifteen years and supports the VLT back end of currently sixteen instruments.

The ESO VLT QC service requires a data reduction system with a pipeline that generates master calibrations with quality control parameters that either measure the quality of the pipeline product (e.g. signal-to-noise ratio of the master flat) or the quality of the instrument or of a component of the instrument (e.g. spectral resolution).

Quality control parameters are extracted from the pipeline products, ingested in a public database and used for trending and scoring[4,7,8] .

At the time of writing the SPHERE data reduction pipeline is incomplete and consequently a considerable part of the data reduction cascade is not in operation. Therefore the challenge in the first year of SPHERE operations is not to handle the complexity of the instrument but to achieve a minimum level of quality control without having sufficient pipeline support in order to minimize the areas where the instrument would be operated blindly otherwise. In cases where a functional data reduction recipe is available a quality control script is started after the pipeline processing in order calculate quality control parameters thereby compensating for fragmentariness of the data reduction system.

Furthermore the knowledge transfer from the consortium to the operations has not been completed. This means that operational quality control is expected to find undocumented dependencies of quality characteristics, which have to be isolated in order to distinguish between common cause and assignable cause events in the trending.

We report here on several examples which finally improved instrument operations. Most of the following operational highlight examples are based on quality control parameters calculated by post pipeline processing scripts.

3.1 ZIMPOL DARK CALIBRATIONS

ZIMPOL dark levels of the optical CCDs were showing a bi-modal distribution with maxima at 2 ADU/sec and 7 ADU/sec, predominantly present for a specific detector setup. After several investigation, the problem was successfully identified as a temporal long-term accumulation of dark counts in case the optical CCD wasn't read out for a longer time ($t > 24h$). This operational feature was improved by starting the day-time calibration batch with a technical read out sequence in order to clean and discharge the optical detectors.

3.2 IRDIS PHOTOMETRIC ZEROPOINTS

The IRDIS calibration plan includes two on sky calibrations: astrometric standard stars and photometric standard stars, which are acquired for efficiency monitoring in four broad bands Y, J, H and K. Both calibrations are not yet pipeline supported. Photometric standard stars are acquired in closed AO loop and without coronograph in order to provide in addition to the throughput of the IRDIS arm also the Strehl ratio as a performance parameter of the adaptive optics.

Since the throughput is a high priority metric of an instrument we decided to submit the photometric standard star exposures to the IRDIS pipeline science recipe for basic data reduction and analyze the pipeline products per channel of the dual band with the *eclipse peak*[5] command as a temporal solution. The photometric standard star catalog used by the NACO data reduction pipeline is applied to derive the photometric zero points in J, H and K.

Photometric standard stars acquired in the J band use the ND_2.0 neutral density filter located in the CPI, for which a zero point of 19.4 mag can be derived for early 2016. Observations with the H and K band broad band filters use the ND_3.5 neutral density filters, for which zero points of 17.7 mag and 19.2 mag are retrieved respectively. Given both IRDIS beams the photometric zero points differ by 0.04 mag in J, 0.02 mag in H but 0.496 mag in K.

3.3 IRDIS DBI BACKGROUND CALIBRATIONS

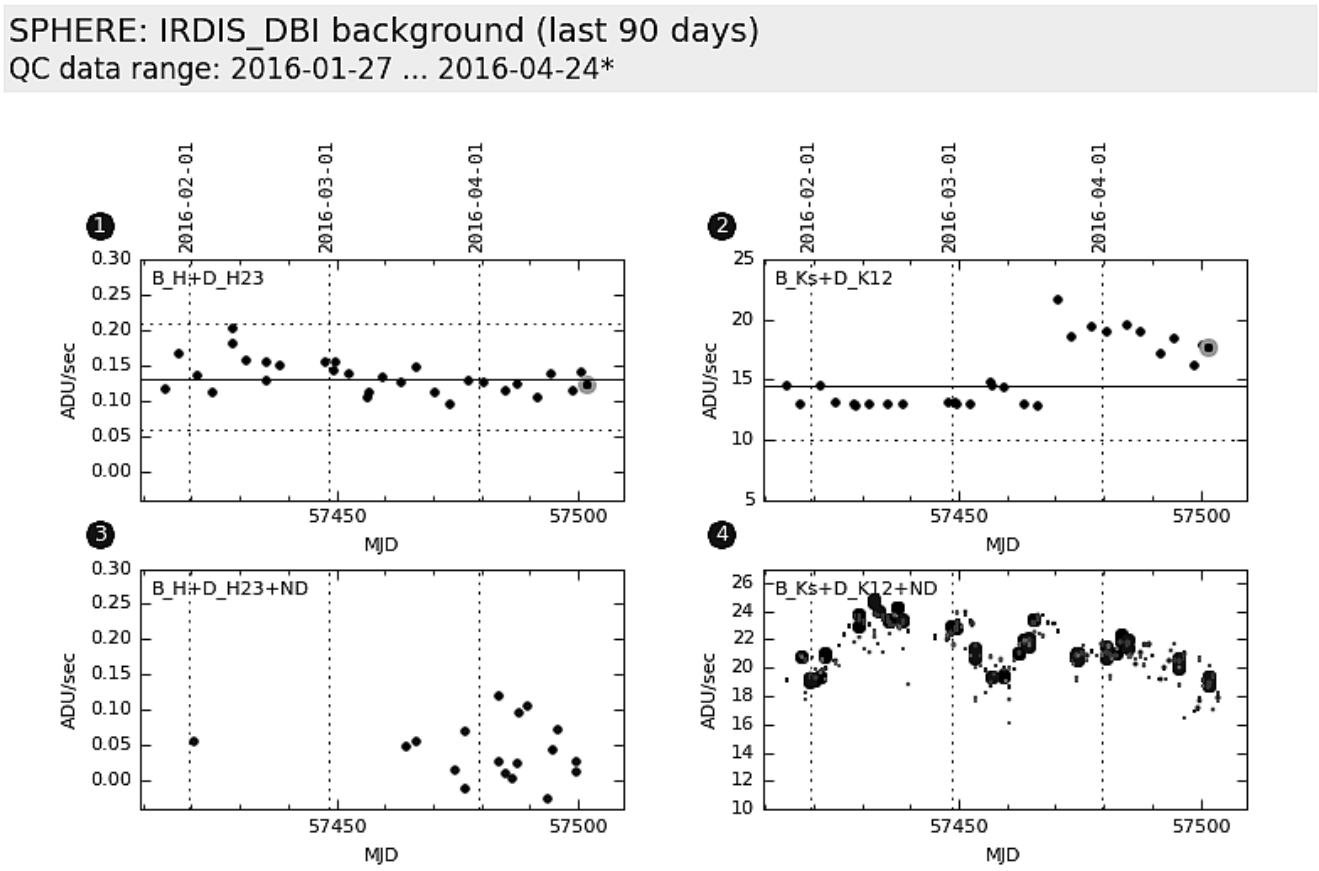

Figure 2. This trending plot collects several dependencies of the IRDIS background radiation. A low and stable background of 0.13 ADU/sec for H-band (box 1), a background value of 13 ADU/sec, stable up to mid March of 2016 (box 2), a low level but higher scatter background in the H band when a neutral density filter is in the optical path (box 3), and a high level and temperature dependent K-band background when a neutral density filter is in the optical path (big symbols in box 4). The small symbols are scaled temperature values.

While earlier NIR instruments calibrate their science data with dark frames, where two narrow band filters without overlap in wavelength act like a radiation shield, IRDIS and IFS use background frames without filters in the optical path, hence collecting not only the isotropic radiation from the detector itself and the radiation through the detector shield but also the radiation component of the whole instrument and the CPI. While this contribution is negligible for Y, J and H bands with about 0.15 ADU/sec (see Fig. 2, box 1), the K band shows several dependencies.

- When there is no neutral density filter in the CPI, the K-band background is rather stable, at least between 2015-07 and 2016-03 with about 13 ADU/sec (box 2 in Fig. 2).
- When there is one of the neutral density filters in the optical path of the CPI, the background is higher by about 22 ADU/sec and it varies with the temperature of the neutral density filter. This behavior is demonstrated in box 4 of Fig. 2 where the K-band background is shown for two neutral density filters (big symbols). The scaled values of two temperature sensors are over plot in box 4 to demonstrate this correlation.

3.4 THERMAL IMPACT ON THE IFS DETECTOR

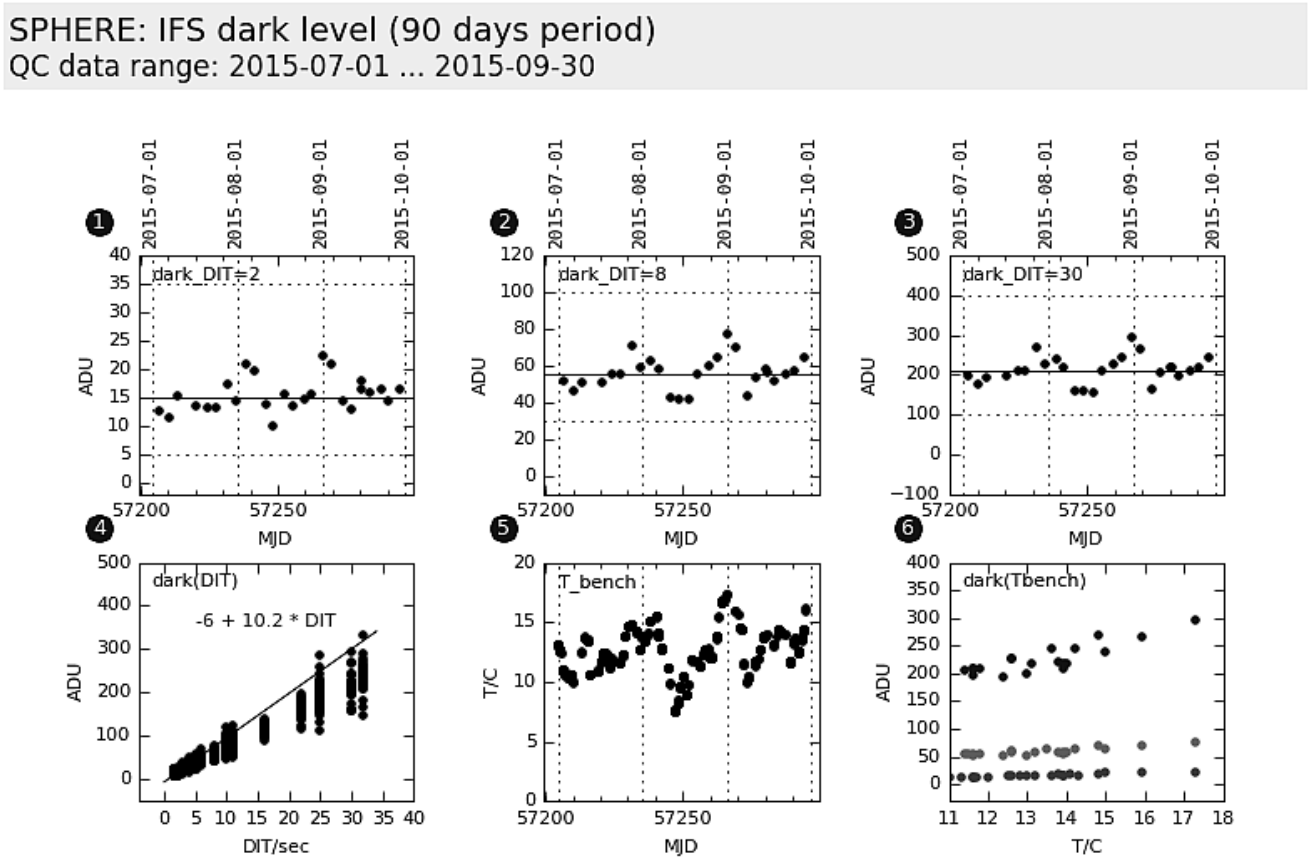

Figure 3. Health Check plot for the IFS detector related QC parameter dark level, showing the expected dependency on the exposure time DIT and the dependency on the IFS bench temperature, which is related to the ambient temperature. The IFS bench temperature is monitored in box 5 and box 6 demonstrates, that the scatter in boxes 1, 2 and 3 is due to variations of the bench temperature. Box 4 shows the dark levels as a function of DIT and together with a best-fit model derived from the first months. The upper dots in box 6 for DIT=30 sec indicate a bi-modal distribution to be investigated.

The two main characteristics of the IFS detector, the dark level and the read out noise show a dependency on the ambient temperature. This was found by a correlation between these quality parameters with the IFS bench temperature sensor. As demonstrated in box 4 of Fig. 3, the dark level shows a linear dependence on the exposure time DIT as expected. Furthermore the IFS bench temperature given in box 5 shows the same pattern as the three trending plots in boxes 1, 2, and 3. Finally box 6 shows the dependency of the dark level on the temperature, here for three different values of DIT=2, 8 and 30 sec for which it is most pronounced. For DIT=30 a bi-modal distribution of the dark level can be read from the plot, a potential subject for further investigations

Since the IFS detector dark level depends on the exposure time and therefore on thermal radiation, the read out noise is expected to show the corresponding relation according the square root law. Box 4 of Fig. 4 shows the statistical noise as function of DIT together with a best-fit covering the data of the first three months of operations only. This demonstrates that the stable read-out noise (extrapolated to DIT=0 sec) is about 2.5 ADU, while the statistical noise derived from the subtraction of two raw dark frames is composed of the read out noise and an exposure time dependent component, which follows the expected photon noise derived from the dark level. The temperature variations in box 5 show the same pattern as the noise variations in boxes 1, 2 and 3. For that reason, as already demonstrated in Fig. 3, box 6 shows the dependence of the noise on the temperature for the three DIT values subject of the monitoring.

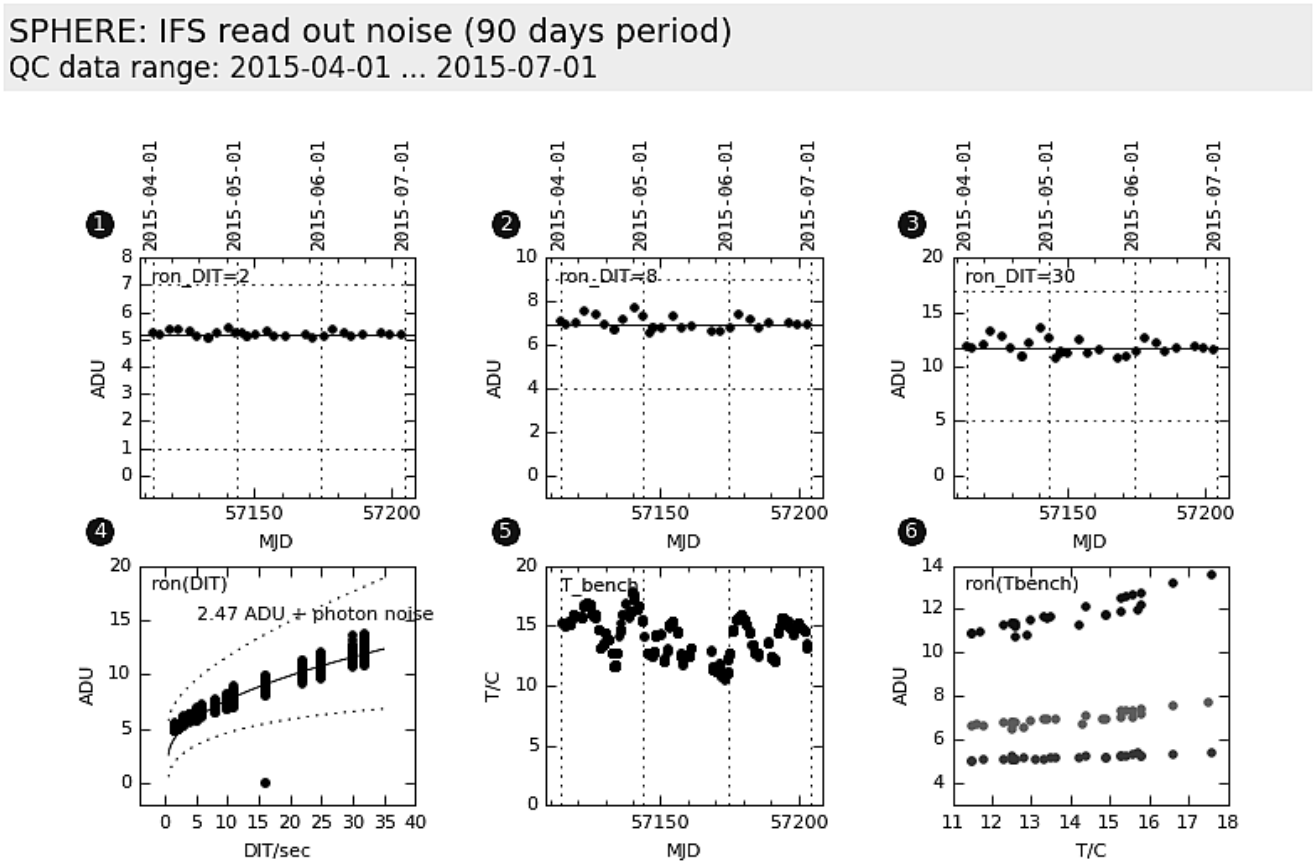

Figure 4. Health Check plot for the IFS detector related QC parameter: statistical noise, which is composed by the read-out noise of the detector and temperature dependent photon noise. The IFS bench temperature is monitored in box 5 and box 6 demonstrates, that the scatter in boxes 1, 2 and 3 is due to the bench temperature. Box 4 shows the RON as a function of DIT and together with a best-fit model derived from the data covering the first weeks of operations. This demonstrates a RON of 2.5 ADU plus photon noise. The upper dots in box 6 for DIT=30 sec indicate a bi-modal distribution to be investigated.

3.5 IFS SPECTRAL POSITION AND EARTH QUAKE EVENT FROM 2015-11-27

The spectroscopic format of the IFS is monitored via several parameters: The number of found slitlet spectra (see box 1 of Fig. 5), the applied correction scale and the offset of the spectroscopic format as a whole in two directions (boxes 4 and 5). The offset of the spectral format shows a non-linear dependency on the IFS bench temperature for both prisms of which the one for the YJ prism is shown in box 3 of Fig. 5. The period selected for Fig. 5 covers also Nov 27 2015 on which the medium risk earth quake (EQ) affected Paranal observatory. The earth quake caused an offset in the spectroscopic format by 0.8 pixel in x-direction only (perpendicular to

the wavelength direction). The pre-EQ relation is shown as a dashed curve in box 3. The non-linearity of the temperature relation was not affected. Since the trending offset is rather small and since the data reduction pipeline is able to process the post-EQ frames in this case, there is no need for any instrumental realignment. The only consequence concerns data flow operation and is to assure that pre-EQ calibrations are not used to calibrate post-EQ science data and vice-verse.

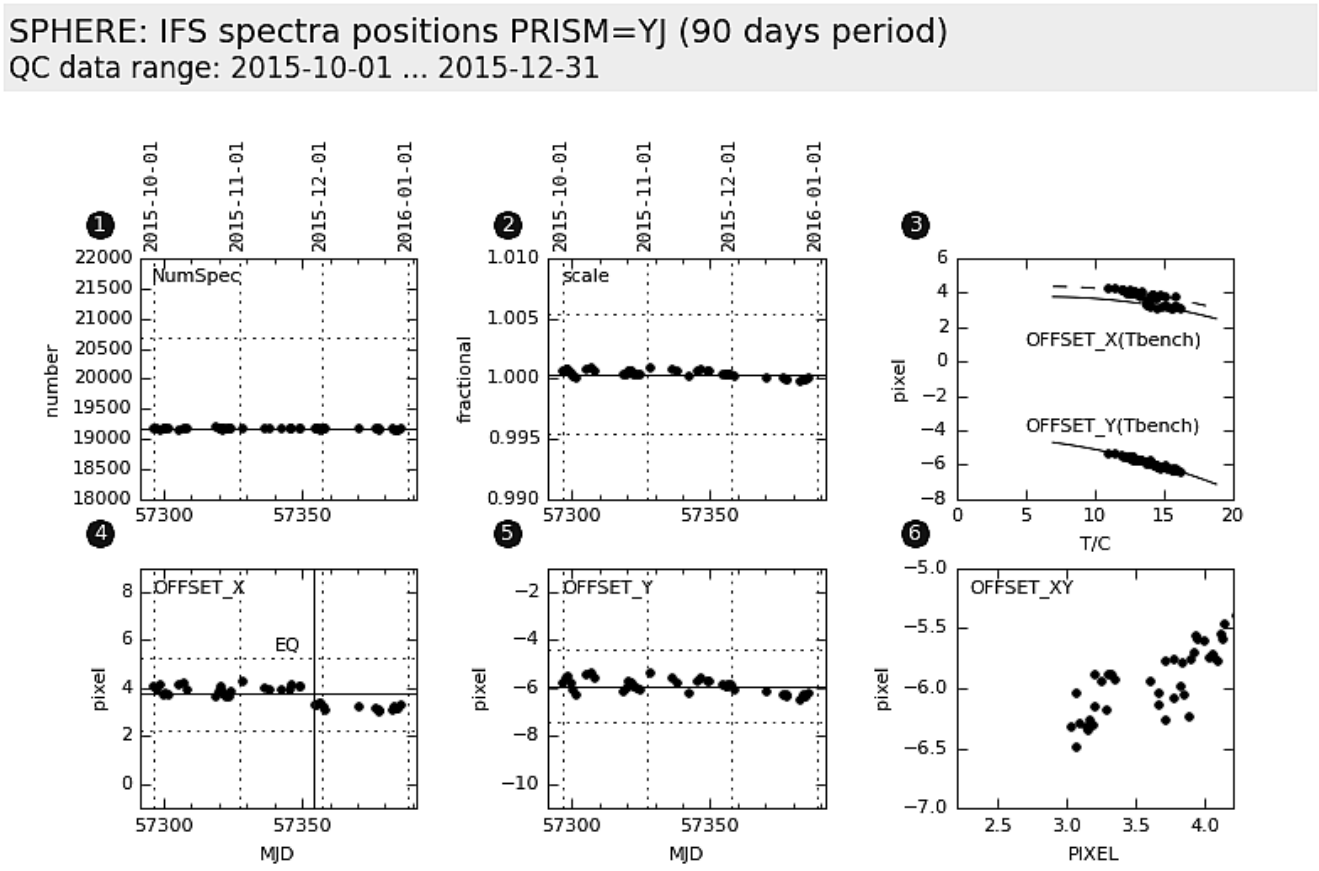

Figure 5. This health check plot covers the main quality control parameters retrieved from the IFS spectral position recipe, the number of detected and used spectra, the correcting scale applied, and the spectral format position in terms of offset values in both directions. Box 3 shows the non-linear dependence of both offset directions from the IFS bench temperature. A highlight is the resolved shift of the spectral mask position of 0.6 pixel after the earth quake event on 2015-11-27.

3.6 FULL PLOTS

After one year of SPHERE operations we started to implement so-called full plots, for the most critical instrumental parameters covering not only the last three months for day-to-day quality control, but covering the full lifetime of the instrument in order to find long-term trends. These long term trends can identify aging effects like that of calibration lamps and coatings of optical components that result in the replacement or cleaning of instrumental components. Another effect can be slowly moving components that lead to a misalignment and that could be re-adjusted by maintenance or by configuration control. An example with a large time range for the VLT are full plots for UVES that are covering sixteen years of operations. For SPHERE the few full plots cover four hundred days. Fig. 6 shows as an example the ZIMPOL modulation de-modulation efficiency, that is required as a correction factor in the data reduction. The parameter is monitored for two read modes and for the two beams.

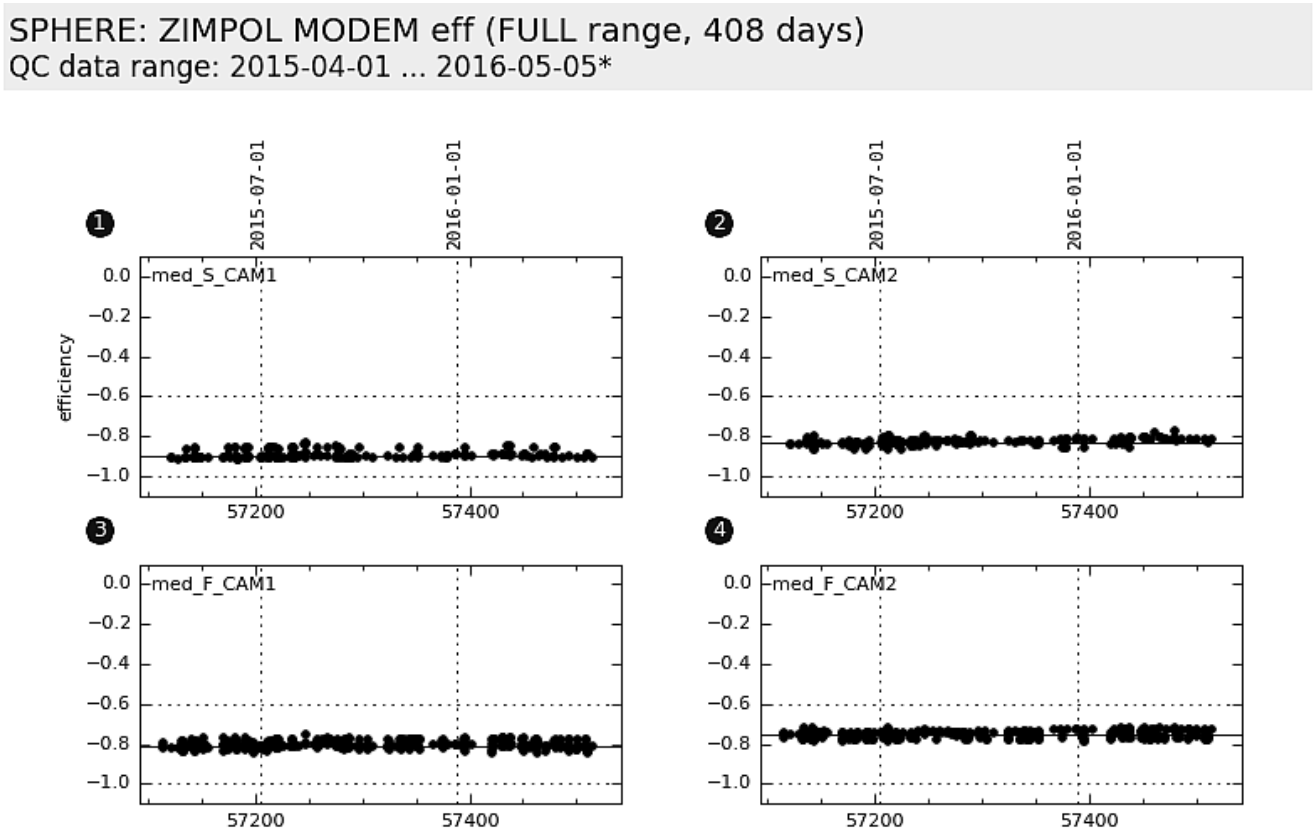

Figure 6. Full lifetime plot to monitor the long term trend of the ZIMPOL modulation demodulation efficiency quality control parameter for both beams (CAM1 and CAM2) and for two read modes (FastPolarimetry and SlowPolarimetry).

4. OUTLOOK

The next steps in completing the QC service plan, as far as they do not depend on the completion of the data reduction pipeline, will focus on the following points.

- After having identified several unexpected dependencies of the instrument quality characteristics on parameters which are not under control (e.g. the ambient temperature) we intend to monitor parameters cleaned for these known biases in order to increase the contrast and thereby the detection probability for potential assignable causes like single outliers from the mean and changes of the mean itself.
- Several calibration templates like the IFS gain template suffer from generating sub-optimal calibration frames. We intend to improve these calibration sequences.

ACKNOWLEDGMENTS

We would like to thank Sabine Möhler and Melissa McCure for sharing the results of their pipeline tests and Burkhard Wolff for extending the *DFO raw_display* tool to handle fits data cubes.

REFERENCES

[1] Beuzit, J.-L.; Feldt, M.; Dohlen, K. et al., "SPHERE: a 'Planet Finder' instrument for the VLT" in [*Ground-based and Airborne Instrumentation for Astronomy II.*], McLean, I. S.; Casali, M. M. Loew, M. H., ed., *Proc. SPIE* **7014**, 7014E (2008).

[2] Zampieri, S., Chuzel, O., Ferguson, N. et al., "OCA - A Flexible Rule Engine for Data Organisation, Classification & Association", ADASS XV ASP-CS, Vol. **351**, 196, 2006

[3] W. Freudling, M. Romaniello, D.M. Bramich et.al., "Automated data reduction workflows for astronomy", A&A **559**, A96, 2013

[4] Wolff, B.; Hanuschik, R.W.; Hummel, W.; et al., "Solutions for quality control of multi-detector instruments and their application to CRIRES and VIMOS", in [*Observatory Operations: Strategies, Processes, and Systems II.*], Brissenden, R.J.; Silva, D.R. ed., *Proc. SPIE* **7016** 70160S, (2008)

[5] Devillard, N. "ESO C Library for an Image Processing Software Environment (eclipse)", ADASS X ASP-CS, Vol. **238**, 525, 2002

[6] Mawet, D., Girard, J., Wahhaj, Z., et al., "SPHERE User Manual" VLT-MAN-SPH-14690-0430-v95, P95.2, 2015

[7] Hanuschik, R., "Distributed Quality Control of VLT Data at ESO", ADASS XVI ASP-CS, Vol. **376**, 373, 2007

[8] Hanuschik, R.W.; Neeser, M.; Hummel, W. et al., "Scoring: a novel approach toward automated and reliable certification of pipeline products", in [*Observatory Operations: Strategies, Processes, and Systems II.*], Brissenden, R.J.; Silva, D.R. ed., *Proc. SPIE* **7016** 70160Q, (2008)